Article

Root Uptake of Lipophilic Zinc#Rhamnolipid Complexes

Samuel P. Stacey, Michael J. McLaughlin, Ismail Çakmak, Ganga M. Hettiarachchi, Kirk G. Scheckel, and Michael Karkkainen

J. Agric. Food Chem., **2008**, 56 (6), 2112-2117 • DOI: 10.1021/jf0729311 • Publication Date (Web): 28 February 2008

JOURNAL OF AGRICULTURAL AND FOOD CHEMISTRY

Root Uptake of Lipophilic Zinc−Rhamnolipid Complexes

SAMUEL P. STACEY,*,† MICHAEL J. MCLAUGHLIN,†,‡ ISMAIL ÇAKMAK,§ GANGA M. HETTIARACHCHI,‡ KIRK G. SCHECKEL,# AND MICHAEL KARKKAINEN‡

Soil and Land Systems, School of Earth and Environmental Sciences, The University of Adelaide, PMB 1, Glen Osmond, SA 5064, Australia; CSIRO Land and Water, PMB 2, Glen Osmond, SA 5064, Australia; Faculty of Engineering and Natural Sciences, Sabanci University, 81474 Tulza, Istanbul, Turkey; and National Risk Management Research Laboratory, U.S. Environmental Protection Agency, Cincinnati, Ohio 45224-1702

This study investigated the formation and plant uptake of lipophilic metal−rhamnolipid complexes. Monorhamnosyl and dirhamnosyl rhamnolipids formed lipophilic complexes with copper (Cu), manganese (Mn), and zinc (Zn). Rhamnolipids significantly increased Zn absorption by *Brassica napus* var. Pinnacle roots in ^{65}Zn-spiked ice-cold solutions, compared with $ZnSO_4$ alone. Therefore, rhamnolipid appeared to facilitate Zn absorption via a nonmetabolically mediated pathway. Synchrotron XRF and XAS showed that Zn was present in roots as Zn−phytate-like compounds when roots were treated with Zn-free solutions, $ZnSO_4$, or Zn−EDTA. With rhamnolipid application, Zn was predominantly found in roots as the Zn−rhamnolipid complex. When applied to a calcareous soil, rhamnolipids increased dry matter production and Zn concentrations in durum (*Triticum durum* L. cv. Balcali-2000) and bread wheat (*Triticum aestivum* L. cv. BDME-10) shoots. Rhamnolipids either increased total plant uptake of Zn from the soil or increased Zn translocation by reducing the prevalence of insoluble Zn−phytate-like compounds in roots.

KEYWORDS: Chelate; fertilizer; lipophilic; rhamnolipid; zinc

INTRODUCTION

Worldwide, millions of hectares of arable land are deficient in plant available trace elements such as copper (Cu), iron (Fe), manganese (Mn), and zinc (Zn). Trace element deficiencies affect both global food production and human nutrition and health. The World Health Report (2002) ranked Zn and Fe deficiencies fifth and sixth, respectively, among the 10 leading risk factors for the development of illness and diseases in developing countries. Fertilizer usage is the most rapid and practicable solution to trace element deficiencies in soils and crops, with positive effects for human nutrition (*1, 2*).

On alkaline soils, adsorption and precipitation reactions can substantially reduce the efficacy of trace element fertilizers. For over 60 years, chelating agents such as ethylenediaminetetraacetic acid (EDTA) and diethylenetriaminepentaacetate (DTPA), among others, have been used to increase the persistence of trace elements in the soil solution or for direct application to plant foliage. Physiological studies have shown that metal EDTA and DTPA complexes are not readily absorbed by plant roots (*3–5*). Therefore, dissociation of the chelate complex in the rhizosphere is required prior to trace element absorption, as specified by the Free Ion Activity Model (*6, 7*). The chelants, EDTA and DTPA, form very stable anionic complexes with trace element cations, which explains why chelation reduces cationic metal absorption by plants grown in solution culture (*3–5*). However, Halvorson and Lindsay (*3*) hypothesized that metal−chelate complexes dissociate in the rhizosphere to restore equilibrium as free metal ions are absorbed by the root. Furthermore, a metal ion could exchange the extracellular chelant for a root transport ligand (*8*), if the stability of the metal−chelate complex is less than that of the metal−transport ligand. Thus, in trace element deficient soil, the rate-limiting step for trace element absorption may be governed by the dissociation kinetics of the metal−chelate complex (*9*). If the dissociation kinetics proceed slowly, or if root binding sites or ion carriers cannot dissociate the metal−chelate complex, these chelates may hinder metal absorption from the rhizosphere. In theory, chelates that facilitate metal absorption by roots could provide a more efficient supply of trace element ions to plants, assuming that the chelate also alters the solid phase speciation of the metal ion or improves soil solution concentration and/or the diffusion of the metal ion to the rhizosphere.

Rhamnolipid is a biosurfactant produced by *Pseudomonas* bacteria. Six structural forms of rhamnolipid have been de-

* Author to whom correspondence should be addressed (telephone +61 8 8303 7284; fax +61 8 8303 6511; e-mail samuel.stacey@adelaide.edu.au).
† The University of Adelaide.
‡ CSIRO Land and Water.
§ Sabanci University.
# U.S. Environmental Protection Agency.

10.1021/jf0729311 CCC: $40.75
Published on Web 02/28/2008

scribed, two of which are produced commercially and were used in this study: R1 monorhamnosyl and R2 dirhamnosyl rhamnolipids (*10*). Rhamnolipids complex a wide range of metal ions and have been used to complex and remove heavy metals from contaminated soils (*11–13*). As a biosurfactant, rhamnolipids contain both hydrophobic and hydrophilic functional groups. The hydrophilic carboxylate group is the primary site responsible for complex formation with metal ions. At the inception of this study we hypothesized that rhamnolipids would form neutral lipophilic complexes with cationic metal ions that would enhance absorption of micronutrient metals by plant roots. The complex's affinity for hydrophobic phases could be facilitated by the presence of the hydrophobic functional groups. This study investigated the absorption of zinc−rhamnolipid by canola roots in solution culture, the effect of rhamnolipid on Zn speciation and distribution in these roots using synchrotron-based spectroscopies, and the response of bread and durum wheats to rhamnolipid application on a calcareous soil from central Anatolia in Turkey.

MATERIALS AND METHODS

The Jeneil Biosurfactant Co. (Saukville, WI) supplied a 25% rhamnolipid liquid extract that contained both R1 ($M_r = 504$) and R2 ($M_r = 650$) rhamnolipids. Subsamples of the rhamnolipid extract were digested in concentrated HNO_3 and analyzed by inductively coupled plasma atomic emission spectroscopy (ICP-AES, Spectroflame, Spectro Analytical Instruments GmbH & Co, Kleve, Germany) to determine the concentrations of contaminant ions. The extract contained negligible Cu, Mn, phosphorus (P), and Zn and was used in the glasshouse trial without further purification.

Separation of R1 and R2 Rhamnolipids Using Column Chromatography. Rhamnolipids R1 and R2 were separated from the crude extract by column chromatography (*10*). Separation was undertaken using a column packed with 50 g of silica gel 60 (Merck, 0.04–0.063 mm) mixed into a slurry with chloroform.

Five grams of crude rhamnolipid extract was dehydrated in an oven at 60 °C, dissolved in 10 mL of chloroform, and loaded into the column using a Pasteur pipet. The column was flushed with chloroform until neutral lipids were completely eluted. Separation was undertaken using three chloroform/methanol mobile phases: 500 mL of 50:3 chloroform/methanol, 500 mL of 50:5 chloroform/methanol, and 200 mL of 50:50 chloroform/methanol at a flow rate of 1 mL/min. Twenty milliliter fractions were collected and then evaporated to dryness under nitrogen gas at 70 °C. The dried rhamnolipid was rehydrated in 8 mM KOH solution. Rhamnolipid fractions were further diluted with Milli-Q water before being directly infused into a mass spectrometer (TSQ Quantum Discovery Max-triple quadrupole, Thermo Fisher Scientific, Waltham, MA) to measure the relative abundance of the R1 and R2 rhamnolipids in each separated fraction. The mass spectrometer conditions were as follows: source, negative electrospray ionization (ESI); full scan mode in Q1; spray voltage, 4300 V; sheath gas, 11 arbitrary units.

The concentrations of R1 and R2 rhamnolipids in the recovered fractions were measured using the method described by Chandrasekaran and BeMiller (*14*) for 6-deoxyhexose sugars. A standard solution was prepared by dissolving 40 mg of L-rhamnose in 100 mL of water. Aliquots of the L-rhamnose standard (0–0.1 mL in 20 μL increments) were transferred to test tubes and made up to 1 mL with deionized water. In addition, 5 and 10 μL of the separated R1 and R2 solutions were transferred to test tubes and made up to 1 mL with deionized water. Sulfuric acid, 4.5 mL of 85% acid solution, was added to each test tube before they were heated in boiling water for 10 min. The tubes were cooled in cold water before 0.1 mL of thioglycolic acid solution (0.1 mL of thioglycolic acid diluted to 3 mL with water) was added. The test tubes were mixed well and then kept in the dark for 3 h. Absorbance was measured at a wavelength of 400 nm using a UV-1601 spectrophotometer (Shimadzu Corp., Kyoto, Japan). A standard curve of L-rhamnose concentration versus absorbance was used to determine the concentration of R1 and R2 in the rhamnolipid solutions. The absorbance calibration curve consistently followed the relationship ($R^2 = 0.93$)

$$\text{Abs } 400 \text{ nm} = 0.3265 + 12.656 \times \text{L-rhamnose(mg/mL)} \quad (1)$$

***n*-Octanol/Water Partition Coefficients.** Five milliliter solutions containing 1 mM $ZnSO_4 \cdot 7H_2O$, $CuSO_4$, and $MnSO_4 \cdot 5H_2O$ and 0.17 mM R1 or 0.60 mM R2 were prepared in 15 mL polyethylene tubes. One milliliter of *n*-octanol was added to the surface of each solution before the vials were sealed and shaken end-over-end for 24 h. Following shaking, 1 mL of solution was removed from the water phase and digested in concentrated HNO_3. The concentrations of Cu, Mn, and Zn in the digest solutions were measured by ICP-AES. All treatments were replicated four times. The concentrations of Cu, Mn, and Zn partitioned in the *n*-octanol phase were determined by mass balance.

The partition coefficient was calculated according to the equation

$$K_{o/w} = \frac{C_o}{C_w} \quad (2)$$

where C_o and C_w refer to the concentration of each trace element ion in the *n*-octanol and water phase, respectively (*15*).

Absorption Kinetics. Canola seedlings (*Brassica napus* var. Pinnacle) were pregerminated on filter paper moistened with deionized water. On day 6, the seedlings were transferred to complete nutrient solution and moved into the glasshouse. The nutrient solution contained Ca (3.55 mM), Mg (1.45 mM), NO_3^- (8.1 mM), $H_2PO_4^-$ (0.2 mM), Cl (10 μM), Na (1.1 mM), K (1.2 mM), SO_4 (1.45 mM), H_3BO_3 (30 μM), MoO_4^{2-} (0.2 μM), Fe-EDDHA (25 μM), Mn (10 μM), Zn (1 μM), and Cu (1 μM), buffered at pH 6.0 with 2 mM 2-morpholinoethanesulfonic acid, 50% as sodium salt (MES) (*16*). After 14 days, the canola plants, three per pot, were transferred to pretreatment solution for 24 h. Pretreatment solution contained 2 mM Na−MES (pH 6.0) and 0.5 mM $CaCl_2$.

Pretreated canola seedlings were transferred to ice-cold and 20 °C uptake solutions containing 2 mM MES, 50% as sodium salt (pH 6.2), 0.5 mM $CaCl_2$, and 5 μM $ZnSO_4$ as either the metal salt or complexed with 5 μM EDTA, 10 μM R1, or 10 μM R2 rhamnolipid. Uptake solutions were spiked with ^{65}Zn to give 0.037 MBq/L. Each treatment was replicated in triplicate. Geochem-PC modeling was used to estimate the free Zn^{2+} activities in each of the uptake solutions. Rhamnolipid stability constants were obtained from published values and were assumed to be similar for R1 and R2 rhamnolipids (*17*).

After 30 min, the canola roots were removed from the uptake solutions and rinsed with Milli-Q water and then transferred to ice-cold desorption solutions for 30 min to desorb the majority of apoplastically bound Zn. Desorption solutions contained 2 mM Na−MES (pH 6.0), 5 mM $CaCl_2$, and 20 μM $ZnSO_4$. The concentration of K^+ remaining in the uptake solutions was measured using ICP-OES. Potassium efflux was used to test for potential loss of membrane integrity due to the presence of chelating agents in the uptake solutions.

Canola plants were separated into roots and shoots, blotted dry, and weighed. Roots were transferred into radioactivity counting vials, to which 4 mL of 5 M HNO_3 was added. Samples were left overnight to solubilize the cell contents before the ^{65}Zn contents of the desorbed roots were measured by gamma spectroscopy (1480 Wizard, Wallac, EG&G Co., Turku, Finland).

Synchrotron μ-X-ray Fluorescence and μ-X-ray Absorption Spectroscopy. Canola plants (*B. napus* var. Holly) were grown in a hydroponic nutrient solution that contained Ca (1 mM), N (5 mM), P_2O_5 (0.28 mM), K (1.06 mM), Mg (0.62 mM), S (0.63 mM), and Fe (17.9 μM). Plants were grown in a controlled environment growth chamber under metal halide and sodium vapor lights, illuminated for 16 h per day to simulate approximately 1100 μmol m^{-2} s^{-1} of photosynthetically active radiation (PAR) with an average temperature of 25 °C. After 2 weeks, the nutrient solution was topped up with deionized water to Zn-starve the plants. Ten days later the canola plants were transferred to pretreatment solution for 24 h.

Following pretreatment, canola roots were transferred to Zn treatment solutions containing 5 μM Zn, either as $ZnSO_4$ or complexed with

Table 1. Percentages of Zn Species in Canola Roots at Selected Zn Hotspots Determined by Linear Combination Fitting of k^2-Weighted μ-XAS Spectra

root treatment	phytate (%)	rhamnolipid (%)	glutamate (%)	lysine (%)	$ZnSO_4$ (%)	χ^{2a}
no Zn	70		23.1	6.9		0.612
$ZnSO_4$	87				13	0.713
Zn−EDTA	75.6		24.4			3.567
Zn−rhamnolipid A	16.7	55.3			28	0.332
Zn−rhamnolipid B	12.4	87.6				0.557

[a] $\chi \Sigma[(\text{fit} - \text{data})/\epsilon]^2/(N_{\text{data}} - N_{\text{components}})$ is the reduced chi-square statistic. The sum is over N_{data} points (98 data points between 3 and 8 k space), and $N_{\text{components}}$ is the number of components in the fit (either 2 or 3 as indicated in the table). The total percentage was constrained to be 100% in all fits. Typical uncertainties in the percentages listed for each standard component are 5%.

EDTA or rhamnolipid. Treatment solutions were buffered at pH 6.0 with 2 mM MES (50% as potassium salt).

After 24 h, roots were separated from canola plants and frozen in liquid N_2. Roots were freeze cut, and thin cross sections were mounted in aluminum holders between two sheets of Kapton film. The distribution of Zn in root thin sections was mapped using X-ray fluorescence at beamline 13-BM (GeoSoilEnviro Consortium of Advanced Radiation Sources) at the Advanced Photon Source, Argonne National Laboratory, Argonne, IL. Samples were carefully inserted into a freezer stage mounted on the rotation axis of an $x-y-\theta$ stepping-motor stage with the Kapton X-ray window facing the beam. Mapping data (μ-XRF) and μ-XAS spectra were collected at a temperature of −30 °C in fluorescence mode with a Ge solid-state 13-element detector (Canberra Industries, Inc.) that allowed simultaneous detection of fluorescence signals from multiple elements. The μ-XRF microprobe at APS beamline 13-BM is capable of collecting fluorescence data with a 15–30 μm beam spot size range (<20 μm resolution) and about 10 mg/kg sensitivity, allowing the study of elements at very low concentration in complex environmental samples.

The area mapped was 1.05 by 1 mm for $ZnSO_4$, 1.7 by 1.4 mm for Zn−EDTA, and 0.9 by 0.8 mm for Zn−rhamnolipid with a step size of 20 μm. At each position, the fluorescence signal from a given element was proportional to the integrated number of atoms of that element along the transect of the synchrotron beam. The sample thickness was approximately 500 μm, that is, greater than the absorption lengths for the fluorescence X-rays of interest; only the upper 100 μm of sample contributed significant fluorescence signal. Zinc XAS spectra were collected at selected hot spots to determine Zn speciation in a spatially resolved manner. For each spot at least triplicate scans covered the range from 175 eV below to 225 eV above the X-ray absorption edge of Zn (~9675 eV). Additionally, XAS spectra were collected for Zn standards including $ZnSO_4$, Zn−EDTA, Zn−rhamnolipid, Zn−citrate, Zn−lysine, Zn−glutamate, Zn−phytate, Zn−proline, and Zn−tyrosine. The Zn XAS spectra for a particular hot spot or standards were averaged. The edge energy was calibrated, the pre-edge was subtracted (by a linear function), and the spectrum was normalized to the second-order polynomial to be equal to one (*18*). The data were then converted to k space (k is the photoelectron wavenumber), weighted with $k = 2$ to compensate for the dampening of the extended X-ray absorption fine structure (EXAFS) amplitude with increasing k space. The k^2-weighted EXAFS spectra for the samples were analyzed by linear combination fitting (LCF) using IFEFFIT software (*19*) for all combinations of the 10 standard spectra. For each root Zn spectra, the combination with the lowest reduced χ^2 was chosen as the most likely set of components in the spot (**Table 1**).

Effect of Rhamnolipid on Trace Element Uptake by Bread and Durum Wheat. Ten bread wheat (*Triticum aestivum* L. cv. BDME-10) or durum wheat seeds (*Triticum turgidum* L. *durum* cv. Balcali-2000) were sown in plastic pots containing 1 kg of clay textured soil [19% sand, 34% silt, 47% clay, 14% total carbonates, pH (H_2O) 8.1, 0.7% organic matter] collected from central Anatolia, Turkey. The soil was known to be Zn-responsive and contained 0.1 mg of DTPA-extractable Zn/kg of soil. The soil was fertilized with a basal nutrient solution containing 200 mg of N/kg of soil as $Ca(NO_3)_2$, 100 mg of P/kg of soil as KH_2PO_4, 20 mg of S/kg of soil as K_2SO_4, and 175 mg of K/kg of soil as KH_2PO_4 and K_2SO_4. Zinc was applied as a $ZnSO_4 \cdot 7H_2O$ solution at 2 mg of Zn/kg of soil mixed with five rates of rhamnolipid biosurfactant, 0, 0.75, 2, 4, and 6 mg/kg, prior to its addition to the soil. Each treatment was replicated three times and arranged in a completely randomized design.

After emergence, plants were thinned to five plants per pot. Wheat plants were grown at Sabanci University under glasshouse conditions in October 2006 for 31 days before shoots were harvested, rinsed in deionized water, oven-dried, and weighed. Ground plant material (0.25 g per sample) was microwave digested in concentrated HNO_3 and analyzed by ICP-OES to determine the nutrient concentrations in harvested shoots. Shoot dry matter production and zinc concentration data were processed by analysis of variance. Least significant difference was calculated to determine whether differences observed between treatment means were significant.

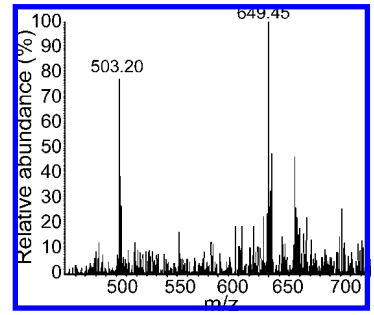

Figure 1. Relative abundance of R1 (m/z 503) and R2 (m/z 649) rhamnolipids in crude rhamnolipid extract.

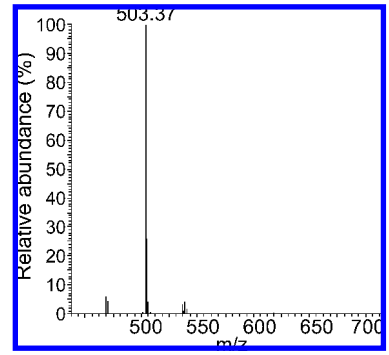

Figure 2. Relative abundance of R1 (m/z 503) and R2 (m/z 649) rhamnolipids eluted in the 50:3 and 50:5 chloroform/methanol mobile phases.

RESULTS

Separation of R1 and R2 Rhamnolipids Using Column Chromatography. The crude rhamnolipid extract contained 48% R1 and 52% R2 rhamnolipids (**Figure 1**). During column chromatography, the R1 rhamnolipid was eluted by the 50:3 and 50:5 chloroform/methanol mobile phases (**Figure 2**) and R2 rhamnolipid was eluted by the 50:50 chloroform/methanol mobile phase (**Figure 3**). Mass spectroscopy (MS) showed that complete separation of the R1 and R2 rhamnolipids was achieved by column chromatography. The mass to charge ratios (m/z) obtained by the MS for R1 and R2 are deprotonated [M − H]$^-$ forms of the rhamnolipids.

***n*-Octanol/Water Partition Coefficients.** Both R1 and R2 rhamnolipids significantly increased the $K_{o/w}$ of Cu, Mn, and Zn ions (**Figure 4**). In the absence of rhamnolipid, polar trace element ions remained in the water phase, that is, $K_{o/w} \approx 0$

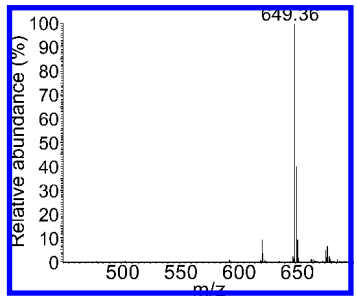

Figure 3. Relative abundance of R1 (*m*/*z* 503) and R2 (*m*/*z* 649) rhamnolipids eluted in the 50:50 chloroform/methanol mobile phase.

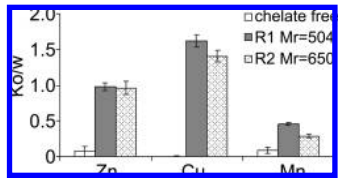

Figure 4. *n*-Octanol–water partition coefficients ($K_{o/w}$) for Zn, Cu, and Mn complexed by R1 and R2 rhamnolipids (±1 SE).

Table 2. Zn Absorbed by Canola Roots over a 30 min Uptake Period

	Zn absorbed[a] (10^{-3} μmol/g of fresh root)		K^+ efflux from roots (μmol/g of fresh root)	
fertilizer	ice-cold	20 °C	ice-cold	20 °C
$ZnSO_4$	3.588 b	5.271 b	1.909	0.386
Zn−EDTA	1.556 a	2.531 a	1.109	0.341
Zn−R1	4.421 c	4.416 b	6.712	4.059
Zn−R2	4.288 c	5.094 b	1.696	0.618

[a] Values within each column with the same letter are not significantly different (LSD $P > 0.05$).

(**Figure 4**). These results showed that both R1 and R2 rhamnolipids were responsible for the formation of lipophilic complexes with these trace elements.

Absorption Kinetics. Geochem-PC was used to estimate Zn^{2+} activity in the uptake solutions. According to Geochem-PC, the free Zn^{2+} activities in chelate free, 5 μM EDTA, and 10 μM rhamnolipid solutions approximated 3.874×10^{-6}, 4.909×10^{-8}, and 3.603×10^{-7}, respectively, at pH 6.2.

EDTA significantly ($P \leq 0.05$) reduced Zn absorption by canola in both ice-cold and 20 °C uptake solutions (**Table 2**). Type R1 and R2 rhamnolipids significantly ($P \leq 0.05$) increased Zn absorption by canola roots in ice-cold solutions compared with $ZnSO_4$ alone and Zn−EDTA. Cold temperatures suppress active absorption pathways in plant roots (*20, 21*). This suggests that R1 and R2 rhamnolipids facilitated Zn absorption via nonmetabolically mediated pathways. At 20 °C, there was no significant difference in Zn absorption between the R1 and R2 treatments and $ZnSO_4$, despite a 10-fold lower Zn^{2+} activity in the rhamnolipid solutions. However, canola roots absorbed significantly more Zn from solutions buffered with R1 and R2 rhamnolipids than those buffered with EDTA.

Potassium efflux from roots was measured to ascertain whether the chelates affected the integrity of the root membranes. High K^+ efflux could indicate that the chelates had a phytotoxic effect at the rates applied. Type R1 rhamnolipid significantly ($P \leq 0.05$) increased K^+ efflux from canola roots in ice-cold and 20 °C solutions (**Table 2**). Neither type R2 rhamnolipid nor EDTA increased K^+ efflux from roots compared with $ZnSO_4$ alone, even though type R2 rhamnolipid significantly increased Zn uptake by canola roots in ice-cold solutions compared with $ZnSO_4$ (**Table 2**). These results suggest that R2 rhamnolipid may have facilitated Zn absorption by intact roots via a nonmetabolically mediated pathway.

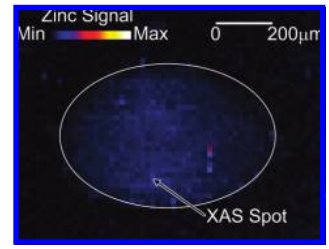

Figure 5. Zinc μ-X-ray fluorescence showing the distribution of Zn in a canola root treated with Zn−EDTA.

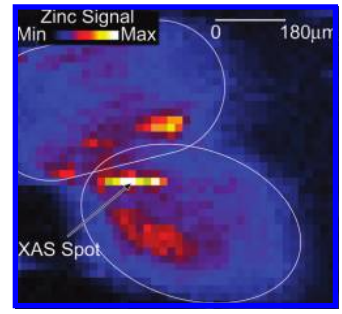

Figure 6. Zinc μ-X-ray fluorescence showing the distribution of Zn in a canola root treated with $ZnSO_4$.

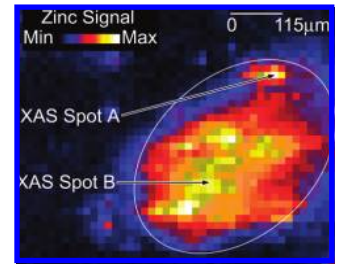

Figure 7. Zinc μ-X-ray fluorescence showing the distribution of Zn in a canola root treated with Zn−rhamnolipid.

Synchrotron μ-X-ray Fluorescence and μ-X-ray Adsorption Spectroscopy. Variations in signal intensity from synchrotron μ-X-ray fluorescence (XRF) demonstrated relative changes in the spatial distribution of Zn within root cross sections; white or yellow colors indicate high Zn concentrations, whereas blue or black colors indicate low Zn concentrations (**Figures 5**−**7**). The lowest Zn μ-X-ray fluorescence signal was obtained from the Zn-EDTA treated roots (**Figure 5**). This was probably due to a reduction in Zn absorption by roots due to low solution Zn^{2+} activities in the presence of EDTA (**Table 2**). The Zn signal was higher in $ZnSO_4$-treated roots and highest in zinc−rhamnolipid roots (**Figures 6** and **7**). Micro X-ray absorption spectroscopy (XAS) suggested that Zn was predominantly in the form of zinc−phytate-like compounds in Zn-free and $ZnSO_4$- and Zn-EDTA treated roots, with 70–87% of total root Zn present as zinc−phytate-like compounds in these treatments (**Table 1**). Zn−EDTA complexes were not detected inside root cross sections. This was consistent with published literature that showed Zn−EDTA complexes were not readily absorbed by intact roots via active or passive uptake pathways (*3–5*). In roots treated with Zn−rhamnolipid, μ-XAS suggested that 55.3 and 87.6% of Zn was probably in the form of Zn−rhamnolipid at spots A and B, respectively (**Figure 7**; **Table 1**). Zinc−phytate-like compounds were less prevalent, 16.7 and 12.4% of Zn at spots A and B, respectively (**Table 1**). These results suggest

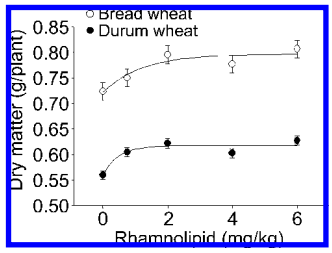

Figure 8. Bread and durum wheat dry matter response to rhamnolipid. Bars denote least significant difference ($P \leq 0.05$).

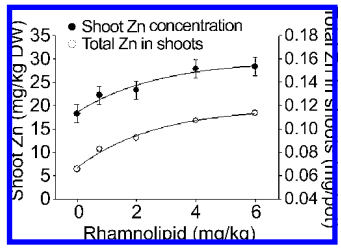

Figure 9. Effect of rhamnolipid shoot Zn concentration and total shoot Zn in bread wheat. Total shoot Zn accounted for dilution due to dry matter responses. Bars denote least significant difference ($P \leq 0.05$).

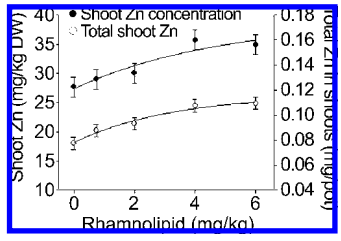

Figure 10. Effect of rhamnolipid on shoot Zn concentration and total shoot Zn in durum wheat. Total shoot Zn accounted for dilution due to dry matter responses. Bars denote least significant difference ($P \leq 0.05$).

that Zn−rhamnolipid complexes may have been absorbed intact by roots, which may have been possible due to the lipophilic properties of these complexes.

Effect of Rhamnolipid on Trace Element Uptake by Bread and Durum Wheats. Rhamnolipid biosurfactant significantly ($P \leq 0.05$) increased dry matter production of both bread and durum wheat (**Figure 8**). Dry matter responses were recorded at application rates of up to 2 mg of rhamnolipid/kg of soil (**Figure 8**). In addition, the concentrations of Zn in wheat shoots significantly increased with rhamnolipid application at rates of up to 4 mg of rhamnolipid/kg soil (**Figures 9** and **10**). The total concentrations of Zn in the soil were identical between treatments. Therefore, rhamnolipid facilitated Zn absorption by roots and/or the translocation of Zn in wheat plants.

DISCUSSION

The column chromatography method used in this study achieved complete separation of R1 and R2 rhamnolipids. During column chromatography, Sim et al. (*10*) used 2.5 times less 50:5 chloroform/methanol mobile phase than we used in this study. The 50:5 chloroform/methanol mobile phase was largely responsible for eluting the R1 monorhamnosyl surfactant. This probably explains why the R2 dirhamnosyl fraction collected by Sim et al. (*10*) contained 5% monorhamnosyl surfactant.

Available data in the literature suggest that lipophilic compounds, such as rhamnolipid−metal complexes, can be readily absorbed across biological membranes, including plant roots, via a hydrophobic pathway (*8, 22–24*). Briggs et al. (*25*) found that lipophilic pesticides were more readily absorbed by barley roots than polar nonlipophilic compounds. Phinney and Bruland (*26*) showed that lipophilic chelates facilitated Cu, cadmium, and lead absorption by coastal diatoms, whereas nonlipophilic chelates, including EDTA, impaired metal absorption. In addition, Bell et al. (*23*) found that roots of Swiss chard absorbed uncharged $M-EDTA^0$ complexes more readily than polar $M-EDTA^{1-}$ or $M-EDTA^{2-}$ complexes.

In this study, both R1 and R2 rhamnolipids were responsible for the formation of lipophilic complexes with Cu, Mn, and Zn. As expected, the magnitude of the *n*-octanol/water partition coefficients reflected published metal−rhamnolipid stability constants (*17*) and the Irving−Williams order (*27*), which follows the order Cu > Zn > Mn (**Figure 4**). These observations provided further evidence that the degree of lipophilicity was dependent on the level of complex formation with rhamnolipid.

Rhamnolipids R1 and R2 significantly increased symplastic Zn uptake from ice-cold solutions even though the Zn^{2+} activity was lower than in the chelate-free control. Cold temperatures suppress active absorption pathways in plant roots (*20, 21*), which explains why root absorption of $ZnSO_4$ was low in ice-cold solutions. In active roots, ionic Zn is thought to be transported by ATP-powered proteins embedded within the root membrane (*28, 29*). Therefore, these results suggest that Zn−rhamnolipid complexes were absorbed via a nonmetabolically mediated pathway, possibly by diffusion as hypothesized by Gutknecht (*22*) and Hudson (*8*). However, R1 did increase K^+ efflux from roots, which may suggest that partial membrane degradation occurred, thereby possibly allowing passive Zn influx. R2 rhamnolipid was not rhizotoxic at the rates applied, but still significantly increased Zn absorption compared with Zn−EDTA and $ZnSO_4$ alone, the latter treatment having a 10-fold higher Zn^{2+} activity than the R2 treatment.

Synchrotron μ-XAS showed that intact Zn−rhamnolipid complexes were likely absorbed by canola roots. These results were consistent with Zn uptake rates from ice-cold solutions, which also suggested that rhamnolipid facilitated Zn absorption via a nonmetabolically mediated pathway, probably due to the lipophilic properties of Zn−rhamnolipid. Rhamnolipid appeared to alter the speciation of Zn inside canola roots by reducing the prevalence of Zn−phytate-like compounds. Thus, the increased Zn concentrations in wheat shoots from the soil study may have been due to an increase in total Zn absorption with rhamnolipid application and/or an increase in Zn translocation due to the formation of more labile forms of Zn inside plant roots.

Rhamnolipid application to soil significantly increased the efficacy of soil-applied Zn, measured as increased dry matter production and increased Zn concentrations, in both durum and bread wheat shoots. Rhamnolipid was effective at low application rates; significant dry matter responses and increased shoot Zn concentrations were measured at application rates of up to 2 and 4 mg of rhamnolipid/kg of soil, respectively. No dry matter response was observed above 2 mg of rhamnolipid/kg of soil because the shoots contained adequate Zn, between 25 and 30 mg of Zn/kg on a dry weight basis (*30*). Results from this study showed that Zn−rhamnolipid complexes were readily plant-available in both solution culture and soil. Despite the relatively low stability constants of Zn−rhamnolipid complexes compared with Zn−EDTA (*17, 31*), the Zn−rhamnolipid complexes appeared to persist long enough in the calcareous soil to have a beneficial effect on plant growth. The fate of rhamnolipid in plants and the persistence of Zn−rhamnolipid complexes in soils will be investigated in future studies.

ABBREVIATIONS USED

EDTA, ethylenediaminetetraacetic acid; XAS, X-ray absorption spectroscopy; XRF, X-ray fluorescence.

ACKNOWLEDGMENT

We thank Caroline Johnston, Atilla Yazici, and Steven Sutton for technical support and Matt Newville for support and useful suggestions for sample setup and synchrotron data collection.

LITERATURE CITED

(1) Cakmak, I. Plant nutrition research: priorities to meet human needs for food in sustainable ways. *Plant Soil* **2002**, *247*, 3–24.
(2) Cakmak, I.; Kalayci, M.; Ekiz, H.; Braun, H. J.; Kilinc, Y.; Yilmaz, A. Zinc deficiency as a practical problem in plant and human nutrition in Turkey: a NATO-science for stability project. *Field Crops Res.* **1999**, *60*, 175–188.
(3) Halvorson, A. D.; Lindsay, W. L. The critical Zn^{2+} concentration for corn and the nonabsorption of chelated zinc. *Soil Sci. Soc. Am. J.* **1977**, *41*, 531–534.
(4) Malzer, G. L.; Barber, S. A. Calcium and strontium absorption by corn roots in the presence of chelates. *Soil Sci. Soc. Am. J.* **1976**, *40*, 727–731.
(5) Marschner, H. *Mineral Nutrition of Higher Plants*, 2nd ed.; Academic Press: London, U.K., 1995; p 10.
(6) McLaughlin, M.; Smolders, E.; Merckx, R.; Maes, A. *Plant Nutrition for Sustainable Food Production and Environment: Proceedings of the XIII International Plant Nutrition Colloquium*, Sept 13–19, Tokyo, Japan; Kluwer Academic Publishers: Dordrecht, The Netherlands, 1997; pp 113–118.
(7) Parker, D. R.; Pedler, J. F. Reevaluating the free-ion activity model of trace metal availability to higher plants. *Plant Soil* **1997**, *196*, 223–228.
(8) Hudson, R. J. M. Which aqueous species control the rates of trace metal uptake by aquatic biota? Observations and predictions of non-equilibrium effects. *Sci. Total Environ.* **1998**, *219*, 95–115.
(9) Degryse, F.; Smolders, E.; Parker, D. R. Metal complexes increase uptake of Zn and Cu by plants: implications for uptake and deficiency studies in chelator-buffered solutions. *Plant Soil* **2006**, *289*, 171–185.
(10) Sim, L.; Ward, O. P.; Li, Z. Y. Production and characterisation of a biosurfactant isolated from *Pseudomonas aeruginosa* UW-1. *J. Ind. Microbiol. Biotechnol.* **1997**, *19*, 232–238.
(11) Torrens, J. L.; Herman, D. C.; Maier, R. M. Biosurfactant (rhamnolipid) sorption and the impact on rhamnolipid-facilitated removal of cadmium from various soils under saturated flow conditions. *Environ. Sci. Technol.* **1998**, *32*, 776–781.
(12) Tan, H.; Champion, J. T.; Artiola, J. F.; Brusseau, M. L.; Miller, R. M. Complexation of cadmium by a rhamnolipid biosurfactant. *Environ. Sci. Technol.* **1994**, *28*, 2402–2406.
(13) Frazer, L. Lipid lather removes metals. *Environ. Health Perspect.* **2000**, *108*, A320–A323.
(14) Chandrasekaran, E. V.; BeMiller, J. N. Constituent analysis of glycosaminoglycans. In *Methods in Carbohydrate Chemistry*; Whistler, R. L., Wolfrom, M. L., Eds.; Academic Press: New York, 1980; pp 89–96.
(15) Chiou, C. T.; Freed, V. H.; Schmedding, D. W.; Kohnert, R. L. Partition coefficient and bioaccumulation of selected organic chemicals. *Environ. Sci. Technol.* **1977**, *11*, 475–478.
(16) Kupper, H.; Lombi, E.; Zhao, F. J.; McGrath, S. P. Cellular compartmentation of cadmium and zinc in relation to other elements in the hyperaccumulator *Arabidopsis halleri*. *Planta* **2000**, *212*, 75–84.
(17) Ochoa-Loza, F. J.; Artiola, J. F.; Maier, R. M. Stability constants for the complexation of various metals with a rhamnolipid biosurfactant. *J. Environ. Qual.* **2001**, *30*, 479–485.
(18) Ravel, B.; Newville, M. ATHENA, ARTEMIS, HEPHAESTUS: data analysis for x-ray absorption spectroscopy using IFEFFIT. *J. Synchrotron Radiat.* **2005**, *12*, 537–541.
(19) Newville, M. IFEFFIT: Interactive EXAFS analysis and FEFF fitting. *J. Synchrotron Radiat.* **2001**, *8*, 322–324.
(20) Lombi, E.; Zhao, F. J.; McGrath, S. P.; Young, S. D.; Sacchi, G. A. Physiological evidence for a high-afinity cadmium transporter highly expressed in a *Thlaspi caerulescens* ecotype. *New Phytol.* **2001**, *149*, 53–60.
(21) Lasat, M. M.; Baker, A. J. M.; Kochian, L. V. Physiological characterization of root Zn^{2+} absorption and translocation to shoots in Zn hyperaccumulator and nonaccumulator species of *thlaspi*. *Plant Physiol.* **1996**, *112*, 1715–1722.
(22) Gutknecht, J. Inorganic mercury (Hg^{2+}) transport through lipid bilayer membranes. *J. Membr. Biol.* **1981**, *61*, 61–66.
(23) Bell, P. F.; McLaughlin, M. J.; Cozens, G.; Stevens, D. P.; Owens, G.; South, H. Plant uptake of ^{14}C-EDTA, ^{14}C-citrate, and ^{14}C-histidine from chelator-buffered and conventional hydroponic solutions. *Plant Soil* **2003**, *253*, 311–319.
(24) McLaughlin, M. Bioavailability of metals to terrestrial plants. In *Bioavailability of Metals in Terrestrial Ecosystems*; Allen, H. E., Ed.; Society of Environmental Toxicology and Chemistry: Pensacola, FL, 2002; pp 39–68.
(25) Briggs, G. G.; Bromilow, R. H.; Evans, A. A. Relationships between lipophilicity and root uptake and translocation of non-ionised chemicals by barley. *Pestic. Sci.* **1982**, *13*, 495–504.
(26) Phinney, J. T.; Bruland, K. W. Uptake of lipophilic organic Cu, Cd, and Pb complexes in the coastal diatom *Thalassiosira weissflogii*. *Environ. Sci. Technol.* **1994**, *28*, 1781–1790.
(27) Irving, H.; Williams, R. J. P. Order of stability of metal complexes. *Nature* **1948**, *162*, 746–747.
(28) Reid, R. J. Mechanisms of micronutrient uptake in plants. *Aust. J. Plant Physiol.* **2001**, *28*, 661–666.
(29) Grusak, M. A.; Pearson, J. N.; Marentes, E. The physiology of micronutrient homeostasis in field crops. *Field Crops Res.* **1999**, *60*, 41–56.
(30) Reuter, D. J.; Robinson, J. B. *Plant Analysis: An Interpretation Manual*, 2nd ed.; CSIRO: Collingwood, Australia, 1997; pp 248–249.
(31) Martell, A. E.; Smith, R. M. *Critical Stability Constants Vol. 1: Amino Acids*; Plenum Press: New York, 1974.

Received for review October 3, 2007. Revised manuscript received January 16, 2008. Accepted January 22, 2008. This work was supported by Mosaic LLC and the Australian Synchrotron Research Program, which is funded by the Commonwealth of Australia under the Major National Research Facilities Program. For research conducted by U.S. Environmental Protection Agency personnel, the views expressed in this paper do not necessarily represent those of the Environmental Protection Agency. Mention of trade names or commercial products does not constitute endorsement or recommendation for use. Synchrotron-based work was performed at GeoSoilEnviro CARS (GSECARS), Sector 13, Advanced Photon Source at Argonne National Laboratory. GSECARS is supported by the National Science Foundation−Earth Sciences, Department of Energy−Geosciences, the W. M. Keck Foundation, and the U.S. Department of Agriculture. Use of the Advanced Photon Source was supported by the U.S. Department of Energy, Basic Energy Sciences, Office of Science, under Contract W-31-109-Eng-38.

JF0729311